DOI: 10.1002/masy.200651103

High Temperature Semibatch Free Radical Copolymerization of Butyl Methacrylate and Styrene

*Deheng Li, Robin A. Hutchinson**

Summary: High temperature starved feed semibatch solution polymerization is used to produce acrylic resins for automotive coatings. These operating conditions promote secondary reactions that have a strong impact on polymerization rate and polymer molecular weight (MW). This study experimentally investigates high temperature semibatch copolymerization of butyl methacrylate and styrene, a system subject to the combined effect of depropagation and penultimate propagation kinetics. A mechanistic model including these complexities is constructed in Predic®. With the termination rate coefficient fit to the semibatch results and all other coefficients taken from independent experiments, the model provides good predictions of monomer conversion and MW. Various representations of copolymer termination kinetics from the literature are compared to the values fit from experiment.

Keywords: butyl methacrylate; copolymerization; kinetics (polym.); modeling; styrene

Introduction

Acrylic resins for automotive coatings are synthesized from a mixture of monomers selected from the methacrylate, acrylate and styrene families. In order to meet environmental regulations as well as to control polymer composition and molecular weight (MW), the polymer is manufactured under higher temperature and lower monomer concentration conditions to reduce the amount of solvent in the reaction mixture.[1] These conditions, however, promote the occurrence of secondary reactions that have a significant impact on the polymerization rate and polymer structure. High temperature homopolymerizations of butyl methacrylate (BMA) and butyl acrylate (BA) and their copolymerization have been previously studied.[1–3] This work will look at copolymerization of BMA and styrene (ST) under similar high temperature starved-feed conditions.

Free radical copolymerization of methacrylate and styrene has been studied extensively in the past, typically at temperatures <80 °C. It was first demonstrated by Mayo and Lewis[4] that, assuming the selectivity of the free radical is controlled by the identity of the last monomer unit, copolymer composition can be expressed as a function of the relative monomer concentrations and reactivity ratios; propagation in a two monomer system is described by four addition reactions. It was later shown that this representation is incapable of simultaneously representing the copolymer composition and average propagation rate coefficient (k_p) for the methyl methacrylate/styrene system.[5,6] The penultimate propagation model, which also considers the effect of the penultimate unit on the radical reactivity, is required to represent rate. Earlier studies of methacrylate and ST copolymerization have focused on penultimate propagation kinetics at lower temperatures.[5–8] We recently carried out kinetic studies for copolymerization of

---

Department of Chemical Engineering, Dupuis Hall, Queen's University, Kingston, Ontario K7L 3N6, Canada
E-mail: robin.hutchinson@chee.queensu.ca

BMA and ST in the temperature range of 50–150 °C,[9] determining that penultimate propagation kinetics have a strong effect on the copolymer-averaged propagation rate coefficient over the entire temperature range, and that the monomer and radical reactivity ratios are constant (within experimental error) over this temperature interval.

Methacrylates are also known to undergo significant depropagation at elevated temperatures.[10] The study of high temperature semibatch homopolymerization of BMA has shown the importance of depropagation effect on polymerization rate and polymer MW.[1] A strong effect of depropagation on the copolymer composition was also observed for the copolymerization of BMA and BA under starved feed conditions.[3] To better understand the behavior of depropagation in copolymerization, a set of equations has been derived to represent the combined effect of depropagation and penultimate propagation kinetics on copolymer composition and copolymer-averaged propagation rate coefficient.[11] Low conversion experiments for copolymerization of BMA and ST at high temperatures and low monomer concentrations confirm the adequacy of the Lowry Case 1 model to describe depropagation in this binary system;[9] i.e., BMA will only depropagate when another BMA is located in the penultimate position.

In this work, a mechanistic model accounting for these kinetic complexities is formulated, and model predictions are compared to a set of BMA/ST semibatch copolymerizations with varying monomer compositions. With proper treatment of copolymerization termination kinetics, the model provides a good representation of the experimental data set.

Experimental Section

Styrene inhibited with 10–15 ppm of 4-tert-butylcatechol and BMA with 10–55 ppm of methyl ether hydroquinone were purchased from Sigma Aldrich at 99% purity and used as received. TBPA (tert-butyl peroxyacetate) in 75 wt% mineral spirits solution and mixed xylene isomer with boiling point 136–140 °C were also purchased from Sigma Aldrich and used as received.

Semibatch reactions were conducted in an agitated 1 L LabMax reactor system with reflux condenser and automatic feeding and temperature control, as described previously.[3] Addition rates of monomer and initiator solutions to the reactor were controlled by monitoring weight loss of the feed tanks using online balances. The experimental recipes are the same as used for BMA/BA copolymerization:[3] The reactor was charged with 215 g solvent and brought up to the reaction temperature of 138 °C. Monomer mixtures (492 g total) and initiator solution (13.1 g total) were continuously added at a constant rate over 6 hours with initiator fed for an extra 15 minutes; the total initiator charge was 2 wt% of the monomer charge. With such a high initiator level, the effect of inhibitor on rate is negligible.

Molecular weights were measured with a Waters 2960 separation module attached to a Waters 410 differential refractometer (DRI) and a Wyatt Instruments Dawn EOS 690 nm Laser Photometer multiangle light scattering (LS) detector using THF as the eluent at a flowrate of 1 mL min^{-1}. The DRI detector was calibrated with 10 narrow polydispersity polystyrene (pS) standards over a broad MW range (870–355000 Dalton), with values reported according to this pS calibration. The LS detector was calibrated by toluene as recommended by the manufacturer. A Wyatt Optilab DSP refractometer was used to measure the refractive index (d*n*/d*c*) values for the polymers in THF, required to analyze output from the LS detector. The LS results provide a better measure of true MW and are compared against model predictions in this work; MW values from the two detectors (presented later) are within 15% of each other. A Waters CP-3800 gas chromatograph (GC) with a flame ionization detector was employed to measure the free monomer concentration in the samples, with a Chrompack capillary column (CP-Sil 8 CB, 30 m in length and 0.25 mm inside diameter) used for separation.

$$\begin{array}{ll}
P_n^{1\bullet} + M_1 \xrightarrow{P_{11}k_{\mathrm{p}111}} P_{n+1}^{1\bullet} & P_n^{1\bullet} + M_1 \xrightarrow{P_{21}k_{\mathrm{p}211}} P_{n+1}^{1\bullet} \\
P_n^{1\bullet} + M_2 \xrightarrow{P_{11}k_{\mathrm{p}112}} P_{n+1}^{2\bullet} & P_n^{1\bullet} + M_2 \xrightarrow{P_{21}k_{\mathrm{p}212}} P_{n+1}^{2\bullet} \\
P_n^{2\bullet} + M_2 \xrightarrow{P_{12}k_{\mathrm{p}122}} P_{n+1}^{2\bullet} & P_n^{2\bullet} + M_2 \xrightarrow{P_{22}k_{\mathrm{p}222}} P_{n+1}^{2\bullet} \\
P_n^{2\bullet} + M_1 \xrightarrow{P_{12}k_{\mathrm{p}121}} P_{n+1}^{1\bullet} & P_n^{2\bullet} + M_1 \xrightarrow{P_{22}k_{\mathrm{p}221}} P_{n+1}^{1\bullet}
\end{array}$$

Scheme 1.
Penultimate propagation kinetic scheme for binary copolymerization.

Model Development

By establishing material balances on the monomer and initiator, one can qualitatively predict the kinetic behavior of a homopolymerization system in a starved feed reactor under idealized conditions.[12] This two monomer BMA (1)/ST (2) system, however, requires a more detailed mechanistic treatment, including penultimate propagation kinetics and depropagation. The commercial software package, Predici®, which calculates chain-length distributions using a discrete Galerkin technique with variable grid and variable order, offers the capability to implement complex kinetic schemes, as discussed in the previous BMA/BA study.[3] New mechanisms to consider for this work are thermal initiation of styrene, and the penultimate model for chain growth.

It is well known that polymerization of styrene can readily proceed via thermal initiation at higher temperatures (100–200 °C). The mechanism was first proposed by Mayo[13,14] and has been further refined by other researchers.[15] It is generally accepted that styrene monomer first undergoes a reversible Diels-Alder dimerization which leads to the formation of an intermediate product that undergoes molecule induced homolysis to produce two radicals, each capable of initiating polymerization. This mechanism is included in the model, but is not an important radical generating reaction under low monomer concentration starved feed conditions, due to the high rates of radical generation from added initiator.

As shown in our kinetic study of BMA/ST,[9] penultimate propagation kinetics must be considered. For a binary system, there are eight monomer addition reactions when considering the penultimate unit of the radicals, as shown in Scheme 1. To reduce the number of species in the model, two types of chain-end radicals are defined, indicated as $P_n^{1\bullet}$ and $P_n^{2\bullet}$ with n representing chain length. P_{ij} represents the fraction of radical j with i unit present in the penultimate position, and is introduced to track the penultimate unit in a terminal radical. Thus,

$$\begin{array}{ll} P^{11\bullet} = P_{11}P^{1\bullet}, & P^{22\bullet} = P_{22}P^{2\bullet} \\ P^{21\bullet} = P_{21}P^{1\bullet}, & P^{12\bullet} = P_{12}P^{2\bullet} \end{array} \qquad (1)$$

where $P^{j\bullet}$ represents all radicals ending in repeat unit j ($P^{j\bullet} = \sum_{n=1}^{\infty} P_n^{j\bullet}$) and $P^{ij\bullet}$ represents all radicals ending in ij ($P^{ij\bullet} = \sum_{n=1}^{\infty} P_n^{ij\bullet}$). From the definitions, it is clear that $P_{11} + P_{21} = 1$ and $P_{22} + P_{12} = 1$. $k_{p_{ijk}}$ is the rate coefficient for addition of monomer k to radical ij, leading to the following definitions of monomer (r_i) and radical (s_i) reactivity ratios for the implicit penultimate propagation model:[5]

$$\begin{array}{ll} r_1 = k_{p_{111}}/k_{p_{112}} = k_{p_{211}}/k_{p_{212}}; & s_1 = k_{p_{211}}/k_{p_{111}} \\ r_2 = k_{p_{222}}/k_{p_{221}} = k_{p_{122}}/k_{p_{121}}; & s_2 = k_{p_{122}}/k_{p_{222}} \end{array} \qquad (2)$$

Methacrylates undergo significant reversible propagation at temperatures higher than 120 °C,[16] the mechanism having a strong impact on both polymerization rate and polymer MW.[1] The implementation of depropagation in copolymerization has been addressed in detail in the BMA/BA study with regard to terminal propagation kinetics.[3] The depropagation rate coefficient k_{dep} is expressed as the product of the equilibrium monomer concentration $[M]_{eq}$ and the propagation rate coefficient.

$$K = k_{p_{111}}/k_{dep} = 1/[M]_{eq}; \quad k_{dep} = [M]_{eq}k_{p_{111}} \tag{3}$$

with $[M]_{eq}$ a function of temperature T and polymer mass fraction in the reactor, x_{wp}:

$$[M]_{eq} = (1.76 \times 10^6 - 1.37 \times 10^6 x_{wp}) \exp(-6145/T) \tag{4}$$

From our kinetic studies, BMA follows Lowry Case 1 depropagation for the copolymerization of BMA and ST at high temperatures and low monomer concentrations:[9] i.e., depropagation only occurs for the radicals ending with methacrylate unit in both penultimate and terminal positions. When combined with penultimate propagation kinetics, Lowry Case 1 depropagation is represented by Equation (5):

$$P_{n+1}^{1\bullet} \xrightarrow{P_{11}k_{dep}} P_n^{1\bullet} + M_1 \tag{5}$$

The probabilities, also required for the penultimate propagation model (Scheme 1), are calculated by applying the long chain hypothesis and steady state assumption to the radical balances:[11]

$$k_{dep}P_{11}^2 - (k_{p_{211}}[M_1] + k_{p_{112}}[M_2] + k_{dep})P_{11} + k_{p_{211}}[M_1] = 0 \tag{6}$$

$$P_{22} = \frac{k_{p_{122}}[M_2]}{k_{p_{221}}[M_1] + k_{p_{122}}[M_2]} \tag{7}$$

The other reaction steps are as described for the BMA/BA study.[3] Based upon the narrow MWDs obtained experimentally (polydispersities of 1.6 to 2.0), reactions involving dead polymer chains (long-chain branching; reaction of terminal double bonds) are negligible. Tables 1 and 2 summarize all of the mechanisms and kinetic coefficients used in the model, as implemented in Predici.

Table 1.
Kinetic mechanisms of high-temperature butyl methacrylate (1)/styrene (2) copolymerization.

Initiation	$I \xrightarrow{k_d} 2fI^\bullet$ $I^\bullet + M_k \xrightarrow{k_{p_{kkk}}} P_1^{k\bullet}$
Styrene self-initiation	$2M_2 \overset{k_i}{\rightleftharpoons} DA$ $DA + M_2 \xrightarrow{k_i} P_1^{2\bullet} + P_2^{2\bullet}$
Propagation	$P_n^{j\bullet} + M_k \xrightarrow{P_{ij}k_{p_{ijk}}} P_{n+1}^{k\bullet}$
Chain transfer to monomer	$P_n^{j\bullet} + M_k \xrightarrow{k_{tr_{jk}}^{mon}} P_1^{k\bullet} + D_n$
Chain transfer to solvent	$P_n^{j\bullet} + S \xrightarrow{C_{s,j}k_{p_{jjj}}} I^\bullet + D_n$
Termination	
by combination:	$P_n^{j\bullet} + P_r^{k\bullet} \xrightarrow{k_{tc_{jk}}} D_{n+r}$
by disproportionation:	$P_n^{j\bullet} + P_r^{k\bullet} \xrightarrow{k_{td_{jk}}} D_n + D_r$
Depropagation	$P_{n+1}^{1\bullet} \xrightarrow{P_{11}k_{dep}} P_n^{1\bullet} + M_1$

Results and Discussion

Experiments were performed at 138 °C, with a final polymer content of 70 wt% in xylene solution. Monomer compositions (mass ratio) were 100/0, 75/25, 50/50, 25/75, and 0/100 for the set of 5 experiments. The unreacted ST and BMA monomer levels in the semibatch reactor, shown in Figure 1, are low throughout the course of these reactions, a characteristic of starved feed policy. Under these conditions the monomer and polymer compositions remain relatively constant throughout the reactions (Figure 2), illustrating the effectiveness of the starved-feed policy in controlling composition. As instantaneous conversion is kept high, the copolymer composition matches monomer molar feed composition almost exactly, while the monomer composition in the reactor is controlled by the system reactivity ratios. With $r_1 = 0.42$ and $r_2 = 0.61$, the BMA/ST system has an azeotrope composition at $f_{BMA} = 0.4\,(= [BMA]/\{[ST] + [BMA]\})$. Thus BMA is preferentially incorporated into the copolymer at low BMA fraction (f_{BMA} is less than the BMA fraction in the feed), while at high BMA fraction the ST is preferentially incorporated into the polymer so that f_{BMA} is greater than the BMA fraction fed.

Table 2.
Kinetic rate coefficients and model parameters for styrene/butyl methacrylate copolymerization.

	Rate expression	Value at 138 °C	Ref.
Initiation	$k_d(\mathrm{s}^{-1}) = 6.78 \times 10^{-15} \exp(-17714/T)$	1.32×10^{-3}	17
	$f = 0.515$	0.515	1
Styrene self-initiation	$k_1(\mathrm{L \cdot mol^{-1} \cdot s^{-1}}) = 3.5 \times 10^{-7}$	3.50×10^{-7}	18
	$k_i(\mathrm{L \cdot mol^{-1} \cdot s^{-1}}) = 1.633 \times 10^{6} \exp(-12020/T)$	3.25×10^{-7}	19
	$k_f(\mathrm{L^2 \cdot mol^{-2} \cdot s^{-1}}) = 2.19 \times 10^{5} \exp(-13800/T)$	5.73×10^{-10}	20
	$k_{-1}(\mathrm{s}^{-1}) = k_1 k_i / k_f$	–	
Propagation	$k_{p_{111}}(\mathrm{L \cdot mol^{-1} \cdot s^{-1}}) = 3.80 \times 10^{6} \exp(-2754.2/T)$	4.69×10^{3}	21
	$k_{p_{222}}(\mathrm{L \cdot mol^{-1} \cdot s^{-1}}) = 4.266 \times 10^{7} \exp(-3910/T)$	3.16×10^{3}	22
	$r_1 = 0.42,\ r_2 = 0.61;\ s_1 = 0.62,\ s_2 = 0.44$	–	9
Termination	$k_{t_{11}}(\mathrm{L \cdot mol^{-1} \cdot s^{-1}}) = 7.08 \times 10^{9} \exp(-2243/T)$	3.03×10^{7}	31
	$k_{t_{22}}(\mathrm{L \cdot mol^{-1} \cdot s^{-1}}) = 3.18 \times 10^{9} \exp(-958/T)$	3.09×10^{8}	23
	$k_{td_{11}}/k_t = 0.65\ ;\ k_{td_{22}}/k_t = 0.01\ ;\ k_{td_{12}}/k_t = 0.33$	–	
Transfer to solvent	$C_{s,1} = 5.55 \exp(-4590/T)$	7.87×10^{-5}	1
	$C_{s,2}$	1.00×10^{-4}	24
Transfer to monomer	$k_{tr_{11}}^{mon}(\mathrm{L \cdot mol^{-1} \cdot s^{-1}}) = 1.56 \times 10^{2} \exp(-2621/T)$	0.27	1
	$k_{tr_{22}}^{mon}(\mathrm{L \cdot mol^{-1} \cdot s^{-1}}) = 2.31 \times 10^{6} \exp(-6377/T)$	0.427	20
	$k_{tr_{ij}}^{mon}(i \neq j) = k_{tr_{jj}}^{mon} \frac{k_{p_{ij}}}{k_{p_{jj}}}$	–	3
Depropagation	$k_{dep}/k_{p_{111}} = [M]_{eq} = (1.76 \times 10^{6} - 1.37 \times 10^{6} x_{wp}) \exp(-6145/T)$	–	3
Density	$\rho_{\mathrm{BMA}}(\mathrm{kg \cdot L^{-1}}) = 0.91545 - 9.64 \times 10^{-4} T(^\circ\mathrm{C})$	0.782	9
	$\rho_{\mathrm{ST}}(\mathrm{kg \cdot L^{-1}}) = 0.9193 - 6.65 \times 10^{-4} T(^\circ\mathrm{C})$	0.827	
	$\rho_{pol}(\mathrm{kg \cdot L^{-1}}) = 1.19 - 8.07 \times 10^{-4} T(^\circ\mathrm{C})$	1.08	

As monomer and polymer compositions remain constant throughout each experiment, a Mayo-Lewis plot can be constructed from the data set. Figure 3 compares the experimental data to the theoretical predictions by the Mayo-Lewis model[4] (Equation 8) and the Lowry Case 1 depropagation model[11] (Equation 9) with 0.5 mol/L in total monomer concentration ($[M]_{\mathrm{tot}} = [\mathrm{BMA}] + [\mathrm{ST}]$), a value chosen based upon the experimental results shown in Figure 1.

$$F_1 = \frac{r_1 f_1^2 + f_1 f_2}{r_1 f_1^2 + 2 f_1 f_2 + r_2 f_2^2} \tag{8}$$

$$\frac{F_1}{1 - F_1} = \frac{d[M_1]}{d[M_2]} = \frac{[M_1] \sum\limits_{i,j=1}^{2} k_{\mathrm{p_{ij1}}} P_{\mathrm{ij}} [P^{\mathrm{j}\bullet}] - k_{\mathrm{dep}_{11}} P_{11} [P^{1\bullet}]}{[M_2] \sum\limits_{i,j=1}^{2} k_{\mathrm{p_{ij2}}} P_{\mathrm{ij}} [P^{\mathrm{j}\bullet}]} \tag{9}$$

As in Figure 2, F_1 is the mole fraction of repeat unit 1 (BMA) in the copolymer. Radical concentrations $[P^{1\bullet}]$and $[P^{2\bullet}]$are related by Equation (10) and probabilities P_{ij} are defined by Equations (1), (6) and (7).

$$[P^{1\bullet}] = \left(\frac{(k_{\mathrm{p_{221}}} P_{22} + k_{\mathrm{p_{121}}} P_{12})[M_1]}{(k_{\mathrm{p_{212}}} P_{21} + k_{\mathrm{p_{112}}} P_{11})[M_2]} \right) \times [P^{2\bullet}] \tag{10}$$

The composition data are consistent with the previous findings[9] that BMA follows Lowry Case 1 depropagation in copolymerization with ST. However, the effects of depropagation on ST/BMA semibatch copolymerization are smaller than those observed for BA/BMA under identical conditions.[3] This difference results from the alternating tendency of ST/BMA system; with $r_{\mathrm{BMA}} = 0.42$, the occurrence of BMA diads is much less than for the BA/BMA system ($r_{\mathrm{BMA}} = 1.6$).

Although all other rate coefficients are taken from literature, copolymerization k_t values are not available and must be estimated from the experimental data. Due to the lower polymer MWs and high operating temperatures, system viscosity

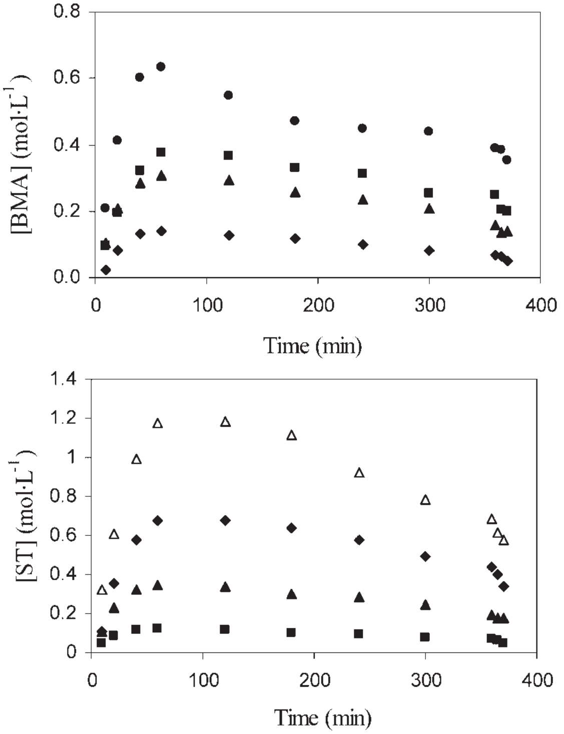

Figure 1.
Butyl methacrylate (top) and styrene (bottom) concentration profiles for semibatch experiments of: ST homopolymerization (△); BMA homopolymerization (●); BMA/ST 75/25 copolymerization (■); BMA/ST 50/50 copolymerization (▲); BMA/ST 25/75 copolymerization (◆).

remains low throughout the semibatch process such that the termination rate coefficient remains under segmental diffusion control and does not appreciably change with monomer conversion.[1,3] Thus, k_t can be considered as a constant for each experiment, but will vary as a function of ST content in the recipe.

The Predici package has a nonlinear parameter estimation toolkit to fit kinetic parameters from experimental results. Based on the mechanistic model summarized in Table 1, BMA and ST concentration profiles were used to estimate copolymerization k_t as a single constant for each experiment. (MW profiles, which are also affected by transfer and mode of termination, were not used in the fit of k_t.) The values were estimated first by assuming terminal propagation kinetics ($s_1 = s_2 = 1$), and then using the model with penultimate propagation kinetics. Figure 4 shows the estimated k_t values vs BMA monomer fraction for the set of experiments, as well as BMA and ST homopolymerization k_t values extrapolated from literature data.[23] The estimated k_t values for homopolymerization are very close to these literature values, validating the model and set of kinetic coefficients as well as the parameter estimation approach. The copolymerization k_t estimates assuming penultimate propagation kinetics are much smaller than the corresponding terminal ones, a behavior also observed by Fukuda et al.[5] for methyl methacrylate/ST copolymerization at 40 °C. Whereas the k_t values for copolymerization estimated assuming terminal kinetics are unreasonably high, the values estimated using penultimate propagation kinetics fall between the homopolymerization values for ST and BMA, as would be

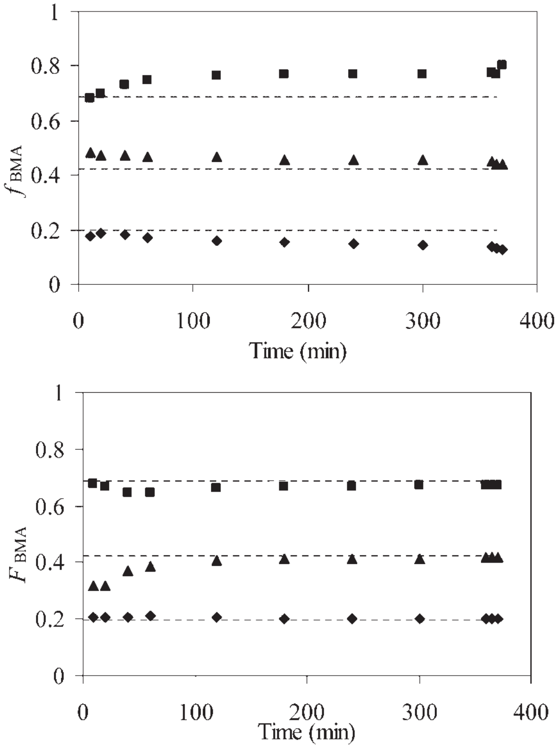

Figure 2.
Monomer fraction (top) and cumulative copolymer composition (bottom) in the semibatch reactions, as determined from GC measurement of residual monomer and calculated by mass balance for the feed ratios (wt%): BMA/ST 75/25 (■); BMA/ST 50/50 (▲); BMA/ST 25/75 (◆). Horizontal lines indicate the monomer feed ratio converted to a molar basis.

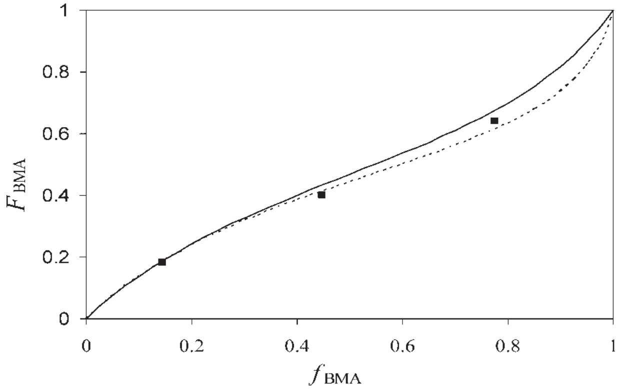

Figure 3.
BMA polymer composition vs monomer composition in the semibatch reactions at 138 °C: experiment (■); Mayo-Lewis model (—); Lowry Case 1 model with $[M]_{tot} = 0.5$ mol/L (- - -).

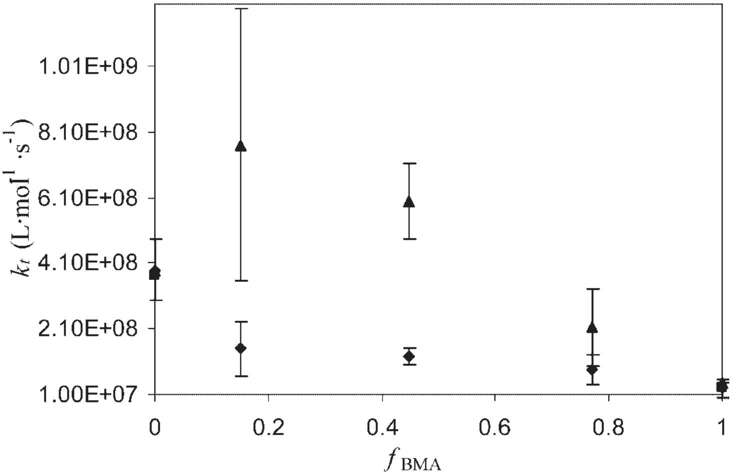

Figure 4.
Termination rate coefficients for BMA/ST copolymerization vs BMA monomer fraction, estimated by assuming terminal propagation (▲) and penultimate propagation (◆) kinetics. Error bar indicates estimated confidence intervals from parameter fitting. Homopolymerization k_t values from the literature (■) are also shown.

expected for this diffusion-controlled rate coefficient. The results in Figure 4 demonstrate the importance of penultimate kinetics for this system, as also shown by k_p measurements.[9]

Figure 5 compares experimental data to the penultimate model predictions using the estimated k_t values. The model provides good predictions for both [BMA] and [ST], and the weight-average polymer MW (M_w) predictions are also reasonable. As it is more difficult to visually compare model vs. experimental MW results, Table 3 summarizes the final M_w values from the DRI and LS detectors and from the model. The polydispersities (M_w/M_n), both experimental and simulated, range from 1.6 to 2.0. The model captures the general increase in copolymer M_w with increasing styrene content, but not the strong dip in M_w observed for the experiment with 75 wt% BMA in the feed relative to BMA homopolymerization. We have no explanation for this experimental finding, which was carefully checked. For all other conditions, simulation values are within 15% of experiment.

There have been various models published in the literature to represent copolymerization k_t. The Walling equation[25] stresses the importance of the terminal unit, as might be expected for a chemically controlled rate coefficient:

$$k_t = k_{t_1} p_1^2 + 2k_{t_{12}} p_1 p_2 + k_{t_2} p_2^2 \tag{11}$$

where p_1 ($=1-p_2$) is the fraction of total radicals that end in monomer 1 calculated from Equation (10), and $k_{t_{12}}$ refers to the cross termination rate coefficient, calculated as the geometric mean of the homopolymerization values. The Atherton and North diffusion model[26] (Equation 12) and Ma's modified diffusion model[27] (Equation 13) emphasize the role of the whole chain composition:

$$k_t = F_1^{inst} k_{t_1} + F_2^{inst} k_{t_2} \tag{12}$$

$$k_t^{-1} = F_1^{inst} k_{t_1}^{-1} + F_2^{inst} k_{t_2}^{-1} \tag{13}$$

Finally, Fukuda and Buback's penultimate termination model[28,29] assumes that copolymerization k_t depends on the conformational characteristics of the last portion of the polymer chain, as represented by terminal and penultimate units:

$$\begin{aligned} k_t^{0.5} = {} & k_{t_{11,11}}^{0.5} p_{11} + k_{t_{21,21}}^{0.5} p_{21} + k_{t_{22,22}}^{0.5} p_{22} \\ & + k_{t_{12,12}}^{0.5} p_{12} \end{aligned} \tag{14}$$

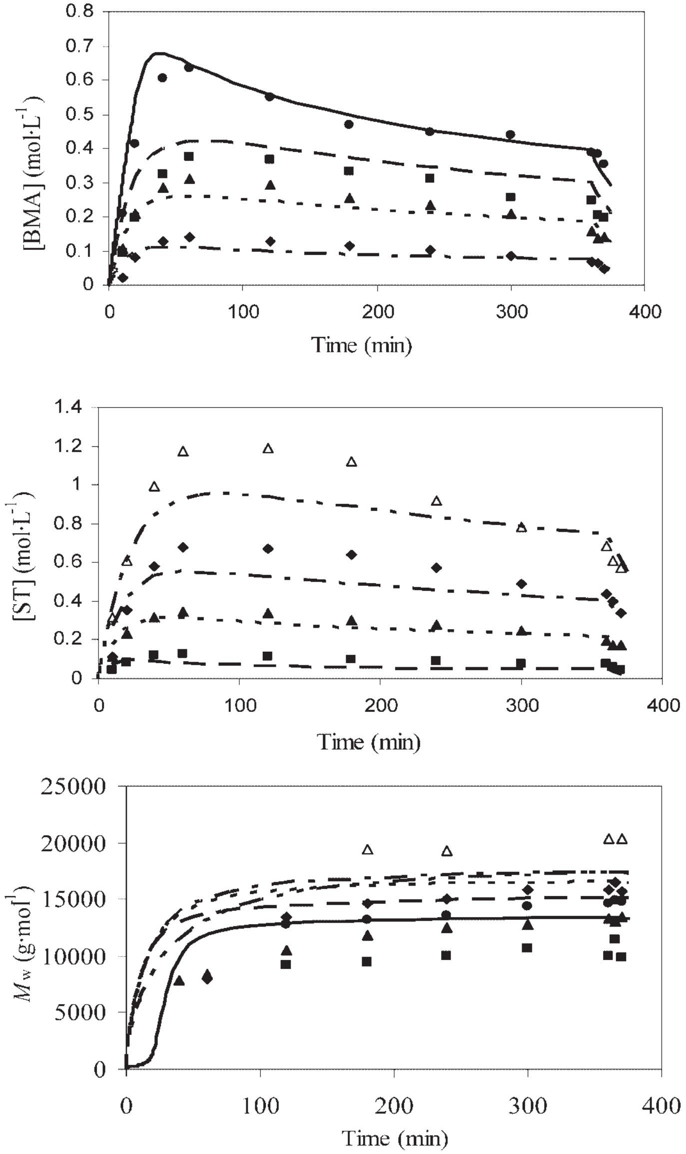

Figure 5.

[BMA], [ST] and weight-average MW model predictions (lines) compared to experimental results (points): BMA homopolymerization (—,●); ST homopolymerization (— - - —, △); BMA/ST 75/25 copolymerization (— —,■); BMA/ST 50/50 copolymerization (- - -,▲); BMA/ST 25/75 (— - —, ◆).

p_{ij} is the fraction of total radicals with repeat units ij at the chain end ($p_{11} + p_{12} + p_{21} + p_{22} = 1$) and $k_{t_{ij,ij}}$ refers to the cross termination rate coefficient between penultimate radicals. Buback et al.[30] used experimental k_t data for acrylate/methacrylate copolymerizations measured by the single-pulse laser polymerization technique to fit $k_{t_{ij,ij}} (i \neq j)$. It was also shown that the data were reasonably represented by a simplified model:[30]

$$\log k_t = f_1 \log k_{t_1} + f_2 \log k_{t_2} \tag{15}$$

Table 3.
Experimental and model predictions of final polymer weight-average MWs.

wt % BMA in the feed	DRI M_w ($g \cdot mol^{-1}$)	LS M_w ($g \cdot mol^{-1}$)	Simulation M_w ($g \cdot mol^{-1}$)
100	12300	14700	13400
75	11500	9800	15200
50	15500	13400	16600
25	17700	15700	17400
0	20600	20400	17400

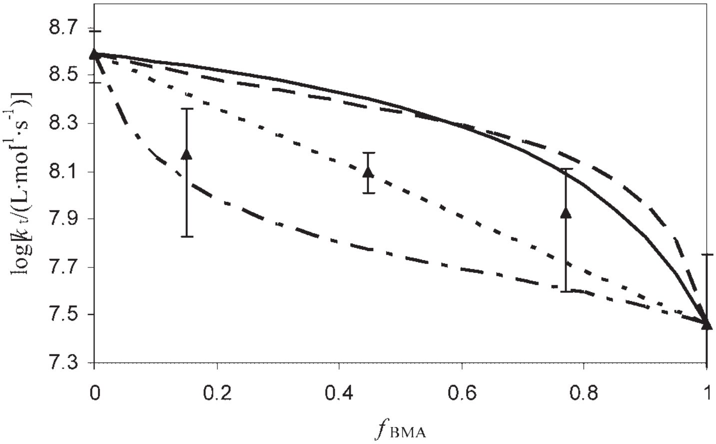

Figure 6.
Termination rate coefficients for BMA/ST copolymerization vs BMA monomer fraction at 138 °C: estimated values (▲); Walling equation (—); Atherton and North model (— —); Buback simplified model (- - -); Ma model (— - —).

With the exception of the Walling representation, all of these models assume copolymerization k_t is not a function of radical type, but is a function of monomer or polymer composition and homopolymerization k_t values. In the absence of experimental copolymerization k_t data for ST/BMA, we examined the ability of the various models to represent the k_t values estimated from our experiments, as shown in Figure 6. The data are best represented by the Buback simplified model (Equation 15) and also reasonably well by Ma's model (Equation 13). While the k_t estimates are not of sufficient accuracy to validate either model, the analysis show the importance of penultimate propagation kinetics for the system and suggests that a relatively simple copolymerization termination model may be adopted for modeling purposes.

Conclusion

A mechanistic model based on implicit penultimate propagation kinetics was formulated for BMA/ST high temperature copolymerization. BMA follows Lowry Case 1 depropagation kinetics, with depropagation having only a slight effect on copolymer composition under the semi-batch conditions. The model, with only one parameter fit, provides a good representation to the experimental data set. Out of several copolymerization k_t models published in the literature, two were able to reasonably represent this system. Future work will extend the copolymerization study to the ternary system consisting of acrylates, methacrylates and styrene.

Acknowledgements: We thank E. I. du Pont de Nemours and Co. and the Natural Sciences and

Engineering Research Council of Canada for financial support of this work.

[1] M. C. Grady, W. J. Simonsick, R. A. Hutchinson, *Macromol. Symp.* **2002**, *182*, 149.

[2] A. N. F. Peck, R. A. Hutchinson, *Macromolecules* **2004**, *37*, 5944.

[3] D. Li, M. C. Grady, R. A. Hutchinson, *Ind. Eng. Chem. Res.* **2005**, *44*, 2506.

[4] F. R. Mayo, F. M. Lewis, *J. Am. Chem. Soc.* **1944**, *66*, 1594.

[5] T. Fukuda, Y. Ma, H. Inagaki, *Macromolecules* **1985**, *18*, 17.

[6] T. P. Davis, K. F. O'Driscoll, M. C. Piton, M. A. Winnik, *J. Polym. Sci., Part C: Polym. Lett.* **1989**, *27*, 181.

[7] M. L. Coote, L. P. M. Johnston, T. P. Davis, *Macromolecules* **1997**, *30*, 8191.

[8] M. L. Coote, M. D. Zammit, T. P. Davis, G. D. Willett, *Macromolecules* **1997**, *30*, 8182.

[9] D. Li, N. Li, R. A. Hutchinson, *Macromolecules* **2006**, *39*, 4366.

[10] S. Bywater, *Tran. Far. Soc.* **1955**, *51*, 1267.

[11] D. Li, J. R. Leiza, R. A. Hutchinson, *Macromol. Theory Simul.* **2005**, *14*, 554.

[12] K. F. O'Driscoll, A. F. Burczyk, *Polym. React. Eng.* **1992**, *1*, 111.

[13] F. R. Mayo, *J. Am. Chem. Soc.* **1953**, *75*, 6133.

[14] F. R. Mayo, *J. Am. Chem. Soc.* **1968**, *90*, 1289.

[15] K. S. Khuong, W. H. Jones, W. A. Pryor, K. N. Houk, *J. Am. Chem. Soc.* **2005**, *127*, 1265.

[16] R. A. Hutchinson, D. A. Paquet, S. Beuermann, J. H. McMinn, *Ind. Eng. Chem. Res.* **1998**, *37*, 3567.

[17] M. Buback, S. Klingbeil, J. Sandmann, M. Sderra, H. P. Vogele, H. Wackerbarth, L. Wittkowski, *Z. Phys. Chem. (Muenchen)* **1999**, *210*, 199.

[18] J. Bonilla, E. Saldivar, A. Flores-Tlacuahuac, E. Vivaldo-Lima, R. Pfaendner, F. Tiscareno-Lechuga, *Polym. React. Eng.* **2002**, *10*, 227.

[19] C. Kotoulas, A. Krallis, P. Pladis, C. Kiparissides, *Macromol. Chem. Phys.* **2003**, *204*, 1305.

[20] A. W. Hui, A. E. Hamielec, *J. Appl. Polym. Sci.* **1972**, *16*, 749.

[21] S. Beuermann, M. Buback, T. P. Davis, R. G. Gilbert, R. A. Hutchinson, A. Kajiwara, B. Klumperman, G. T. Russell, *Macromol. Chem. Phys.* **2000**, *201*, 1355.

[22] M. Buback, R. G. Gilbert, R. A. Hutchinson, B. Klumperman, F. Kuchta, B. G. Manders, K. F. O'Driscoll, G. T. Russell, J. Schweer, *Macromol. Chem. Phys.* **1995**, *196*, 3267.

[23] S. Beuermann, M. Buback, *Prog. Polym. Sci.* **2002**, *27*, 191.

[24] J. Brandrup, E. H. Immergut, E. A. Grulke (Eds.), *Polymer Handbook 4th Edition*, New York: Wiley, **1999**.

[25] C. Walling, *J. Am. Chem. Soc.* **1949**, *71*, 1930.

[26] J. N. Atherton, A. M. North, *Trans. Faraday Soc.* **1962**, *58*, 2049.

[27] Y. D. Ma, T. Fukuda, H. Inagaki, *Macromolecules* **1985**, *18*, 26.

[28] T. Fukuda, N. Ide, Y. D. Ma, *Macromol. Symp.* **1996**, *111*, 305.

[29] M. Buback, C. Kowollik, *Macromolecules* **1999**, *32*, 1445.

[30] M. Buback, C. Kowollik, *Macromol. Chem. Phys.* **1999**, *200*, 1764.

[31] M. Buback, T. Junkers, *Macromol. Chem. Phys.* **2006**, *207*, 1640.